Localized polarons and conductive charge carriers: Understanding $CaCu_3Ti_4O_{12}$ over a broad temperature range

L. Liu,[1] S. Ren,[1] J. Liu,[2] F. Han,[1] J. Zhang,[3] B. Peng,[4] D. Wang,[5,*] A. A. Bokov,[6] and Z.-G. Ye[6]

[1]*College of Materials Science and Engineering, Guilin University of Technology, Guilin 541004, China*

[2]*State Key Laboratory for Mechanical Behavior of Materials, School of Materials Science and Engineering, Xi'an Jiaotong University, Xi'an 710049, China*

[3]*Electronic Materials Research Laboratory-Key Laboratory of the Ministry of Education and International Center for Dielectric Research, Xi'an Jiaotong University, Xi'an 710049, China*

[4]*School of Physical Science & Technology and Guangxi Key Laboratory for Relativistic Astrophysics, Guangxi University, Nanning 530004, China*

[5]*School of Microelectronics & State Key Laboratory for Mechanical Behavior of Materials, Xi'an Jiaotong University, Xi'an 710049, China*

[6]*Department of Chemistry and 4D LABS, Simon Fraser University, Burnaby, British Columbia, Canada V5A 1A6*

(Received 13 January 2019; published 25 March 2019)

$CaCu_3Ti_4O_{12}$ (CCTO) has a large dielectric permittivity plateau near room temperature due to several dynamic processes. Here, we consider the combined effects of localized charge carriers (polarons) and conductive charge carriers using a recently proposed statistical model [Phys. Rev. B **96**, 054115 (2017)] to fit and understand its permittivity measured at different frequencies over a broad temperature range. We found that, at the lowest temperature, the small permittivity is related to frozen polarons, and the increase at higher temperatures is associated with the thermal excitation of polarons that gives rise to the Maxwell-Wagner effect. The final rapid increase at the highest temperature is attributed to thermally activated conductivity. Such an analysis enables us to separate the contributions from localized polarons and conductive charge carriers and quantify their activation energies, which also explains the permittivity plateau near room temperature. In particular, we show that the subtle balance between the number of activated polarons and their polarizability causes CCTO to have a permittivity plateau with small dielectric loss.

DOI: 10.1103/PhysRevB.99.094110

I. INTRODUCTION

Materials with high dielectric permittivity have attracted much attention due to their numerous technological applications. $CaCu_3Ti_4O_{12}$ (CCTO) has a cubic perovskite structure and a giant relative permittivity of 10^4–10^6 near room temperature. While the dielectric permittivity of CCTO exhibits little temperature dependence between 100 and 600 K, it drops rapidly to a value of ∼100 below 100 K [1–10]. This overall behavior of CCTO is very different from either relaxors or normal ferroelectrics. It is established that the origin of the high permittivity near room temperature is an extrinsic effect related to grains and grain boundaries. Therefore polycrystalline CCTO is often modeled after the internal barrier layer capacitor (IBLC), consisting of semiconducting grains separated by thin insulating grain boundaries. Furthermore, the interface effect from electrodes or domain walls is also suggested to contribute to the high permittivity in single crystals.

The remarkable dielectric properties of CCTO also depend on the probing frequency, which approximately follows the Arrhenius behavior. A similar phenomenon was also found in many manganites, cuprates, and nickelates, such as $La_{1-x}Ca_xMnO_3$ [11], $Pr_{0.7}Ca_{0.3}MnO_3$ [12], Tb/$EuMnO_3$ [13–15], $CuTa_2O_6$ [16], $LaCuLiO_4$ [17], $LaSrNiO_4$ [18], Li/Ti-doped NiO [19,20], and $Ba(Fe_{0.5}Nb_{0.5})O_3$ [21–25]. Therefore, a better understanding of CCTO will also help to explain the dielectric properties of a large group of materials. For these materials, their low-temperature dielectric relaxation has been attributed to the hopping of polarons, which are localized charge carriers interacting with phonons [26], between lattice sites with a characteristic timescale. The step-function-like decrease in the permittivity-versus-temperature curve suggests a freezing phenomenon in the relaxation process.

However, some important questions regarding these types of materials remain unanswered. For instance, while it is known that the polaronic relaxation usually involves either a variable-range-hopping (VRH) or a nearest-neighbor hopping conduction process [27,28], an estimation of the activation energy, which is a key parameter for such a process, is still missing. At higher temperatures, the permittivity of such materials also includes the contribution from thermally activated conducting electrons. Meanwhile, the nonlocal conductivity causes a high dielectric loss that increases with the dielectric permittivity at low frequencies. However, it is unclear how important such a contribution is to the total permittivity, which contains the effects of both thermally activated polarons and conductive charge carriers. In fact, for the permittivity of such materials, a complete description of its temperature dependence is unavailable over the temperature range accessible

*dawei.wang@xjtu.edu.cn

to experiments. We note that the Maxwell-Wagner model alone is not enough to describe the permittivity over a broad temperature range [see Eq. (6) below]. In addition, while these materials may be modeled by a parallel *RC* equivalent circuit, resulting in the Arrhenius equation [29], the physics underlying such a phenomenon needs to be understood to establish the connections between the *RC* circuits and the charges and/or dipoles inside. Another remarkable feature of CCTO is its permittivity plateau, which is desirable since it has excellent temperature stability and small dielectric loss. As a matter of fact, such properties have been actively sought and investigated by many researchers [30–32]. However, without knowing the underlying mechanism for the plateau, the search or design of such materials could be shortsighted.

In this paper, we will answer the aforementioned questions using a statistical approach, which is based on macroscopic and phenomenological considerations to decompose the contributions from polarons and conductive charge carriers in CCTO. Using this statistical approach, we propose an explicit formula to fit the permittivity over a broad temperature range, which in turn enables us to separate the contributions from polarons and conductive charge carriers. Such a separation finally allows us to estimate the activation energies of polarons, and conductive charge carriers. Since the analysis separates these two effects and offers some insights regarding them, it helps us explain the permittivity plateau and enhance our understanding of CCTO and similar materials, providing useful clues to design or apply these types of materials.

This paper is organized as the follows. In Sec. II, we show the experimentally obtained dielectric properties of CCTO, which will be analyzed in the following sections. In Sec. III, we propose an explicit formula to fit the permittivity of CCTO over the whole temperature range and use it to analyze the contributions to the permittivity from different origins. In Sec. IV, we discuss the origins that contribute to CCTO's dielectric properties. Finally, in Sec. V, we give a brief summary.

II. EXPERIMENT

$CaCu_3Ti_4O_{12}$ (CCTO) powder was prepared by the molten salt method [33]. The obtained CCTO powder was pressed into pellets of 15 mm in diameter and ∼1 mm in thickness. The pellets were sintered at 1060 °C in the air for 30 h. X-ray diffraction shows that the powder is of pure cubic perovskite phase. Both sides of the samples were first polished and then brushed with silver conductive paste, which is followed by a heat treatment at 550 °C for 30 min. Dielectric measurements were performed with an applied voltage of 500 mV using an Agilent 4294A impedance analyzer over the frequency range of 100 Hz–1 MHz and at temperatures from 90 to 500 K.

A. Dielectric loss

The loss factor of the CCTO sample versus temperature (Fig. 1) shows two regions of large dielectric loss. The Debye-like loss peaks below ∼300 K shift to higher temperatures with the increase of probing frequency, while the other one increases rapidly with temperature, suggesting a thermally activated process.

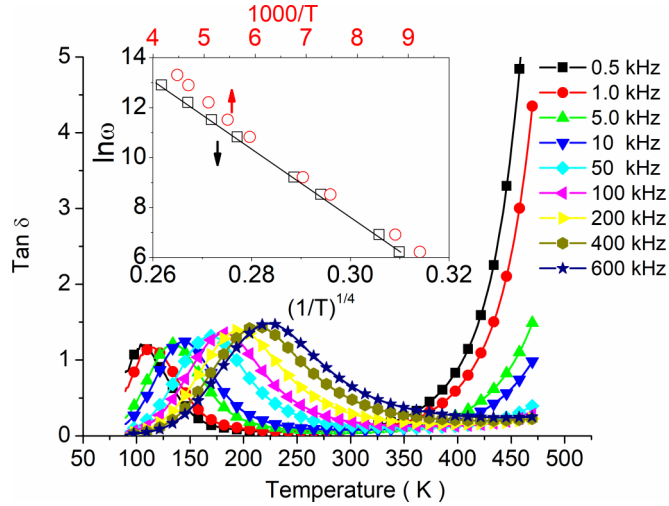

FIG. 1. Temperature dependence of $\tan\delta$ of the permittivity of CCTO at various frequencies. Inset: Temperature-dependent relaxation frequency ω scaled for thermally activated nearest-neighbor hopping of charges (open circles, top and left axes) and VRH (open squares, bottom and left axes). The solid line is the fitting curve of the experimental data (open squares) according to Eq. (1).

To understand the relaxation below 300 K, we first analyze the behavior of the dielectric dissipation. The inset in Fig. 1 shows the temperature dependence of the relaxation frequency of CCTO, $\ln\omega$ vs $1/T^{1/4}$ (open squares), where ω is the position of the loss peak in the $\tan\delta$ vs $\ln\omega$ plots. We can clearly see that there is a good linear relation between $\ln\omega$ and $1/T^{1/4}$.

On the other hand, the plot of $\ln\omega$ as a function of $1000/T$ (open circles) shows an approximate Arrhenius relation. According to this relation, the approaching frequency (when $1000/T = 0$) is 3.59×10^8 Hz and the activation energy 130 meV, respectively. Theses values are in good agreement with those of other perovskite materials [34], related to the localization process of charge carriers. However, it is notable that a deviation from the Arrhenius relation exists above 200 K. Such a deviation has been found in polaron-related relaxations of certain materials, such as CCTO [26,27,35] and $Sr_{0.998}Ca_{0.002}TiO_3$ [36]. The reason for the deviation from the Arrhenius law is likely the transition from a grain-boundary-limited to bulk-limited conduction, consistent with the widely held "barrier layer model" [37,38].

Therefore, according to our results, Mott's variable-range-hopping (VRH) model [39], i.e.,

$$f = f_1 \exp[-(T_1/T)^{1/4}], \tag{1}$$

can better fit the relaxation frequency, where f_1 and T_1 are two constants. The solid line in the inset of Fig. 1 is the fitting result of our experimental data to Eq. (1). The values of f_1 and T_1 are determined to be 1.68×10^{21} Hz and 3.56×10^8 K, respectively. The value of T_1 of CCTO is similar to those of Li-doped La_2CuO_4 [40] and Cu-doped $BaTiO_3$ [41] while f_1 is much higher. According to the IBLC model, the relaxation frequency is related to the dc conductivity and grain-boundary capacitance of CCTO [27], where f_1 has an approximate

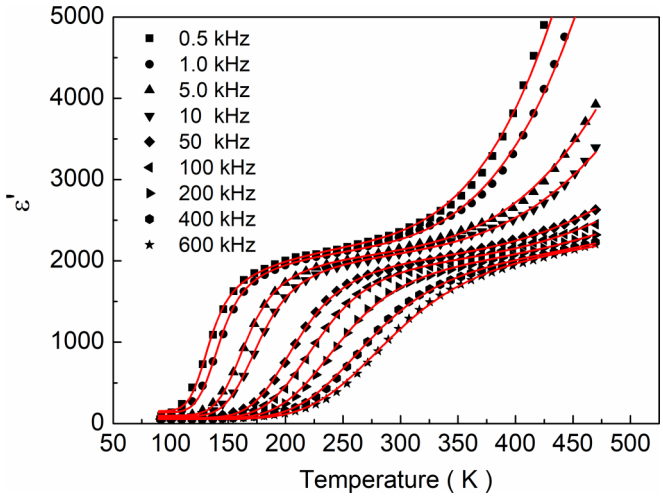

FIG. 2. Temperature dependence of the real dielectric permittivity of the CCTO measured at different frequencies. The solid lines are the fitting results according to Eq. (6).

linear relation with the dc conductivity of the material. Therefore, f_1 does not represent the hopping frequency of polarons.

Since the VRH mechanism describes well the low-temperature dielectric relaxation of CCTO ceramics, it supports the idea that disorder effects dominate the relaxation behavior of CCTO's semiconducting phase. In this phase, the kinetic energy (due to the thermal excitation) is insufficient to excite the charge carrier across the electronic band gap, therefore Eq. (1) is mostly due to the hopping of charge carriers within small regions. Figure 1 thus provides strong evidence for the existence of (hopping) polarons in CCTO.

B. Permittivity

Figure 2 shows the temperature dependence of CCTO's permittivity measured at different frequencies. The rapid increase in the low-temperature region is intimately related to the polaron hopping. Overall, the curves in Fig. 2 have four stages: (i) a region with tiny permittivity at the lowest temperatures (the exact temperature depends on the probing frequency; at 1 kHz, $T < 90$ K), where polarons are frozen and the permittivity is below 100. (ii) As the temperature increases, the dielectric permittivity rises rapidly (at 1 kHz, $90 < T < 150$ K), which is related to the thermal excitation of polarons inside grains. The polaron hopping leads to semiconducting grains, where charge carriers are able to move inside (but not beyond the grain boundaries), resulting in the Maxwell-Wagner effect, which significantly enhances the dielectric permittivity. (iii) A plateau region exists at even higher temperatures (at 1 kHz, $150 < T < 350$ K). (iv) There is another rapid increase of dielectric permittivity at the highest temperatures, which can be attributed to the thermally activated conductivity over the bulk.

Interestingly, Fig. 2 and the above analysis demonstrate some similarities to the temperature-dependent permittivity of relaxors [42], where the contributions to the permittivity from different origins have varying weight over the whole temperature range. As we will show below, the statistical approach adopted in Ref. [42] can also be used to describe the dielectric response of polarons in CCTO.

III. FITTING PERMITTIVITY

To understand the dielectric CCTO's properties over the whole temperature range, it is important to know the the effective permittivity, based on which we can propose a proper formula to fit it.

A. Effective permittivity

The Maxwell-Wagner model can be simplified to consider two slabs representing the grain (g) and grain boundary (gb). The two slabs have a different dielectric permittivity (ε_g and ε_{gb}), conductivity (σ_g and σ_{gb}), and widths (l and d corresponding to the thickness of grains and grain boundaries, respectively, and $L = l + d$). Then, one can obtain the effective permittivity with respect to the frequency ω as [43,44]

$$\begin{aligned}\varepsilon^* &= \frac{L}{l/(\varepsilon_g - i\sigma_g/\omega) + d/(\varepsilon_{gb} - i\sigma_{gb}/\omega)} \\ &= \varepsilon_\infty + \frac{\varepsilon_0 - \varepsilon_\infty}{1 + i\omega\tau} - i\frac{\sigma(\omega)}{\varepsilon_0\omega},\end{aligned} \tag{2}$$

where

$$\begin{aligned}\varepsilon_\infty &= \frac{L}{l/\varepsilon_g + d/\varepsilon_{gb}}, \\ \varepsilon_0 &= \frac{L(\sigma_{gb}\varepsilon_g + \sigma_g\varepsilon_{gb})}{l\sigma_{gb} + d\sigma_g}, \\ \tau &= \frac{l\varepsilon_{gb} + d\varepsilon_g}{l\sigma_{gb} + d\sigma_g}, \\ \sigma(\omega) &= \frac{L\sigma_g\sigma_{gb}}{(l\sigma_{gb} + d\sigma_g)(1 + i\omega\tau)}.\end{aligned}$$

The dielectric permittivity shown in Eq. (2) consists of three contributions. The first term is a constant determined by the permittivity of both the grain and its boundary. The second contribution is of Debye type with the relaxation time determined by the conductivity and permittivity. The third term describes the contribution from the conductivity of grains and grain boundaries.

Equation (2) shows how the dielectric permittivity depends on the properties of grains and grain boundaries within the IBLC model. Since the sizes of the grains and boundaries are difficult to estimate, Abdelkafi *et al.* [45] proposed to use a modified Cole-Cole relaxation by introducing the conductivity to describe the dielectric anomaly of perovskite oxides at high temperature as follows,

$$\varepsilon^* = \varepsilon_\infty + \frac{\varepsilon_0 - \varepsilon_\infty}{(1 + i\omega\tau)^{1-\alpha}} - i\frac{\sigma^*}{\varepsilon_0\omega}, \tag{3}$$

where τ is the mean relaxation time, α is the Cole-Cole parameter, and σ^* ($\sigma^* = \sigma_1 + i\sigma_2$) is the complex conductivity, where σ_1 (σ_2) is due to free charge carriers (space charges within a given region, such as a grain), which suggests that the conductivity contributes to both the real and imaginary parts of the permittivity [46,47].

B. Broad temperature range

Having shown the effective permittivity, we are able to propose a phenomenological model to describe how the permittivity changes with temperature. In this model, individual polarons are categorized into two groups. Our assumption is that the polarons need to be thermally excited to overcome a local energy minimum before they can have large contributions to the grain conductivity σ_g and permittivity ε_g. When the temperature is sufficiently low, most of the polaron charges can only move around their equilibrium positions and their contribution to grain conductivity and permittivity is small and can be taken as a constant. As the temperature increases, while still bounded by grain boundaries, more and more of them can move on a larger spatial scale, jumping from one energy minimum to others, with their contribution to the conductivity and permittivity becoming much larger.

Similar to our statistical model for relaxors [42], here we employ the Maxwell-Boltzmann distribution to estimate the number of active polarons relative to the inactive ones. A potential well of average depth E_b is introduced to account for the constraint on the polarons. Here, the polarons correspond to dipoles in relaxors. Practically, the number of polarons with a kinetic energy exceeding the potential well $[N_1(E_b, T)]$ is given by

$$N_1(E_b, T) = N\sqrt{\frac{4}{\pi}}\sqrt{\frac{E_b}{k_B T}}\exp\left(-\frac{E_b}{k_B T}\right) + N\,\mathrm{erfc}\sqrt{\frac{E_b}{k_B T}}, \tag{4}$$

where N is the total number of polarons in the system, k_B is the Boltzmann constant, T is the temperature (in degrees Kelvin), and erfc is the complementary error function. The total dielectric permittivity is then given by

$$\varepsilon(T, \omega) = \varepsilon_1(T, \omega)P_1(E_b, T) + \varepsilon_2(T, \omega)P_2(E_b, T), \tag{5}$$

where $\varepsilon_1(T, \omega)$ and $\varepsilon_2(T, \omega)$ describe the dielectric responses from the aforementioned two polaron groups, ω is the probing frequency, and $P_1(E_b, T) = N_1(E_b, T)/N$, $P_2(E_b, T) = 1 - P_1(E_b, T)$ account for the proportion of polarons in each group. We note that, according to Eq. (2), the permittivity in Eq. (5) not only results from the intrinsic polarization of polarons, but also the grain conductivity associated with the distribution of the thermally activated polarons, which is often described by the Maxwell-Wagner effect.

Microscopically, the functions $\varepsilon_1(T, \omega)$ and $\varepsilon_2(T, \omega)$ are related to the *polarizability* of each group of polarons. For the "inactive" polarons, $\varepsilon_2(T, \omega)$ can be chosen as a constant, while for the thermally activated polarons, their dynamics under external electric field can be modeled by Debye relaxation, i.e., $\varepsilon_1(T, \omega) \sim 1/(1 + \omega^2\tau_0^2)$ [42,48] was chosen, where τ_0 is the temperature-dependent relaxation time. For a thermally activated process, it follows the Arrhenius law. Consequently, $\varepsilon_1(T, \omega) \sim 1/[1 + A^2\omega^2 \exp(2E_a/T)]$, which was discussed by Jonscher [49] and follows the approach shown in Ref. [42]. In addition to the above analysis, we also need to consider the high-temperature dielectric response induced by the conductivity due to the thermally activated nonlocalized conductive charge carriers [50]. To account for this effect, we use the last term in Eq. (3).

Therefore we propose the following equation to fit the permittivity of CCTO over a broad temperature range,

$$\varepsilon(T) = \frac{\varepsilon_1}{1 + b\exp(-\theta/T)}P_1(E_b, T) + \varepsilon_2 P_2(E_b, T) + \frac{\sigma\exp(-E_{\mathrm{con}}/k_B T)}{\varepsilon_0\omega}, \tag{6}$$

where ε_1, ε_2, b, and θ are constants at a given frequency ω, ε_0 is the vacuum permittivity, σ is the thermally activated conductivity including the contribution from the conductive charge carrier, and E_{con} is the activation energy for the conductive charge carrier's migration and transport. The above equation has clear physical meanings: (i) The first and second terms are the same as in Ref. [42] except that this analysis applies to polarons. (ii) The third term or the right-hand side is the contribution of conductive charge carriers, which is often associated with a thermal activation process.

C. Results from fitting

Having proposed the explicit formula to describe the dielectric permittivity versus temperature, we now use Eq. (6) to fit $\varepsilon(T)$ of CCTO at different frequencies and show the results in Fig. 2 (solid line) where the fitting curves agree well with experimental results.

The fitting results show that the value of E_b exhibits very little dependence on the probing frequency and we find $E_b = 0.19$ eV with a simple averaging procedure and use this value for all the fittings at different frequencies. The activation energy for the conducting charge carriers E_{con} usually relates more to the composition rather than the probing frequency. From our fitting results, $E_{\mathrm{con}} = 0.25$ eV is also obtained by simple averaging. The value of θ is 2100 K, which only slightly changes with the probing frequency.

The fitting in Fig. 2 shows the importance of polaronic conduction in the grains, whose relaxation was likely induced by the charge accumulation at the grain boundaries, which reveals some connections between the polarons and the IBCL model. We also note that the fitting parameters (e.g., E_{con}) depend on samples, especially their grain sizes and composition as discussed in Ref. [33].

To understand the dielectric response of CCTO, we also show $P_1(E_b, T)$, $P_2(E_b, T)$, and the function

$$w_1(T) = \frac{1}{1 + b\exp(-\theta/T)} \tag{7}$$

in Fig. 3(a). Clearly, $P_1(E_b, T)$ and $P_2(E_b, T)$ show little change as the temperature increases, which is different from typical ferroelectric relaxors, such as $Ba(Ti_{1-x}Zr_x)O_3$ for $x > 0.3$, which has a smaller E_b [e.g., $Ba(Ti_{0.6}Zr_{0.4})O_3$ has $E_b = 0.035$ eV] [51]. This feature indicates that the number of "active" polarons which can overcome the potential confinement remains small (P_1 is small) over the experimental temperature range. However, the large value of ε_1 (1.25×10^6–8.97×10^9 depending on the probing frequency, which is much larger than that of typical relaxors) indicates that those polarons are highly correlated and can make an important contribution to the total permittivity once they overcome E_b. The function $w_1(T)$ describes the ability of polarons (which can overcome the potential well) to align with each other

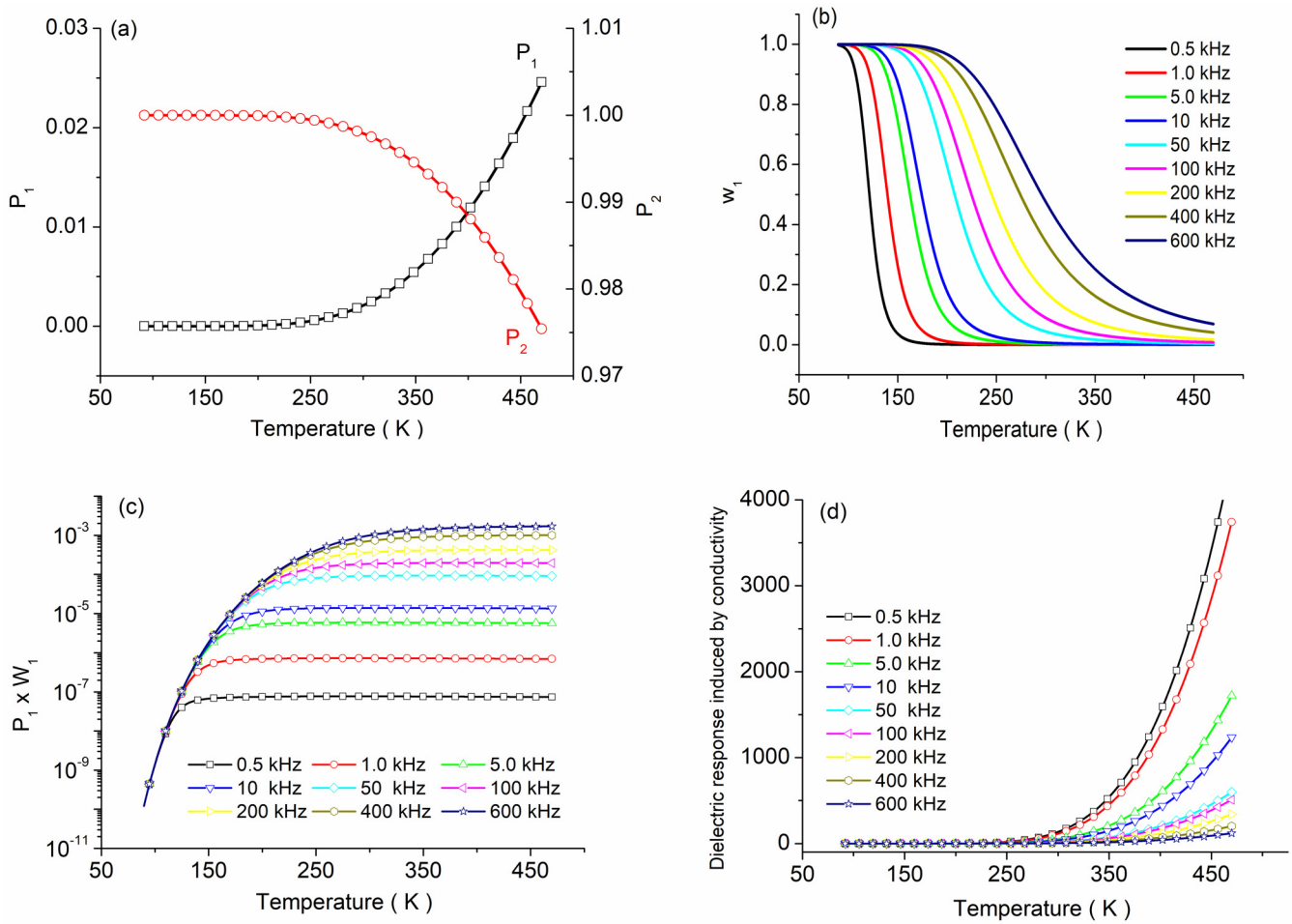

FIG. 3. Decomposition of the contribution to the total permittivity: (a) P_1 and P_2 vs temperature. (b) w_1 vs temperature. (c) $P_1 w_1$ vs temperature shows a rise and a plateau. (d) The dielectric response induced by conductivity.

under thermal fluctuations. Figure 3(b) shows that it is similar to the Fermi-Dirac function, that is, at low temperature the value is close to one but is close to zero at high temperatures.

Figure 3(d) shows the permittivity induced by conductivity [the third term in Eq. (6)]. The contribution of conductivity is small below 200 K but increases rapidly beyond this point. At higher temperatures, due to the thermal activation, conductive charge carriers start to make a large contribution to the dielectric permittivity. At room temperature, the contribution is about 5% of the total dielectric permittivity of CCTO, which suggests that, at room temperature, the Maxwell-Wagner effect induced by thermally activated polarons makes the most important contribution to the total permittivity.

IV. DISCUSSION

In Sec. III, we have shown that separating the contributions to the permittivity enables us to fit it over the whole temperature range. In the following, we discuss the underlying mechanism that makes such a separation necessary and the origin of the permittivity plateau that can be seen in Fig. 2.

A. Polarons and conductive charge carriers

Zhang *et al.* [27] considered that traces of Ti^{3+} exist in CCTO due to the loss of oxygen from the grains during the high-temperature sintering [27], where the Ti^{3+} and Ti^{4+} can form Ti^{3+}-O-Ti^{4+} bonds. The $3d$ electrons in Ti^{3+} ions can thus hop to Ti^{4+} under an applied electric field. Moreover, the formation of Ti^{3+} ions distorts CCTO lattices since the ionic radius of Ti^{4+} is smaller than that of Ti^{3+}, thereby producing a polaronic distortion. The relaxation time of polarons is longer than that of free electrons because of the polaronic distortion.

At low temperatures, polarons stay in more localized states due to the Anderson localization resulting from atom alloying and strain [26]. Therefore, the E_b of CCTO is larger, comparable to that of ferroelectric $Ba(Ti_{0.9}Zr_{0.1})O_3$ ($E_b = 0.24$ eV) and $Ba(Ti_{0.8}Zr_{0.2})O_3$ ($E_b = 0.19$ eV) as discussed in Ref. [51]. In this respect, the dynamic behavior of polarons in CCTO is similar to that in dipoles in normal ferroelectrics. However, the polarization changes in CCTO (due to the hopping of polarons) are conceivably much larger than that of ferroelectrics (due to ion displacements on each lattice site), making the permittivity of CCTO very large. Furthermore, the hopping of charge carriers (polarons) leads to semiconducting

grains, which in turn leads to the Maxwell-Wagner effect. The proposed model here helps us to identify the activation energy, and estimate the relative dielectric strength from different groups of polarons. From this perspective, if we want to increase the polaron contribution, one effective way is to decrease E_b so that more polarons can be excited at room temperature.

It is important to bear in mind that polarons are not the only contribution to the permittivity of CCTO. The conductivity inside the grains increases with temperature (which eventually makes a large contribution to the permittivity at high temperatures). Therefore, the Maxwell-Wagner effect, which results in giant dielectric permittivity, starts to be important at the room temperature (see Fig. 1). By further increasing the temperature, a diffuse dielectric anomaly is observed, because the electrical conductivity with thermally activated electrons from $3d$ electrons in Ti^{3+} ions (the activation energy E_{con} is much lower than that of oxygen vacancies) overcomes the confinement of grain boundaries, becoming high enough to be prominent so as to be included in the last term of Eq. (6). While such effects push the permittivity of CCTO to even larger values, the accompanying dielectric loss is so severe that some balance shall be considered to avoid this situation in the design of practically useful dielectric materials similar to CCTO.

B. Permittivity plateau

Figure 2 shows that, for each probing frequency, the permittivity of CCTO has a plateau region with large values and excellent temperature stability. More importantly, Fig. 1 shows that the plateau regions also have a rather small dielectric loss. These two factors are important in the search for high-permittivity materials with good temperature stability, which are often used as green tapes in the multilayer electronic circuit architecture fabricated using low-temperature co-fired ceramics (LTCC) to enhance functionality and reduce the size of a device [52]. CCTO was also proposed as an alternative dielectric material for multilayer ceramic capacitor (MLCC) applications due to its low sintering temperature, high dielectric permittivity, and temperature stability [31,53]. In fact, CCTO-based compounds with better performance are very attractive for researchers and have been continuously sought. For instance, CCTO-based compounds with $\Delta\varepsilon'$ satisfying the X8R and X9R standards [54] have been reported [55,56]. Consequently, understanding the permittivity plateau shown in Fig. 2 becomes very important for developing such materials. In fact, the results in Fig. 3 reveal the underlying mechanism.

Figure 3(c) shows that for a large temperature range (which depends on the probing frequency), $P_1 w_1$ is essentially a constant. This result is remarkable considering the fact that both $P_1(T)$ and $w_1(T)$ are rather complex functions and some combination of parameters can make $P_1 w_1$ a constant. Figures 3(a) and 3(b) reveal that such combinations do exist in real materials such as CCTO.

Figure 3 also shows that activated polarons are responsible for this permittivity plateau as the first two terms in Eq. (6) are from the contribution of polarons. Interestingly, it can be seen from Figs. 3(a) and 3(b) that, for a large temperature range, the population increase of active polarons exactly compensates their polarizability decrease, giving rise to the permittivity plateau. Since the activation energy for polarons is large (0.19 eV), the increase in P_1 [Fig. 3(a)] is different from the steep increase seen in relaxors [42]. The analysis here indicates that, when making new CCTO-based compounds, the dopants (or alloying components) shall fulfill two conditions: (i) not changing the activation energy of CCTO dramatically (e.g., making it a relaxor by doping), and (ii) not altering the dynamics of active polarons within grains. The ultimate trick is probably to balance P_1 and w_1 perfectly while trying to increase their values.

According to the oxygen vacancy hopping model proposed by Ang *et al.* [57], the long-range motion of charge carriers leads to dc conduction and only contributes to dielectric loss, and the short-range hopping is similar to the reorientation of the dipoles that leads to a dielectric peak. Here, since the polarons are responsible for the permittivity plateau, unlike conductive charge carriers (since they exercise short-range hopping), the dielectric loss due to polaron dynamics is more like in relaxors, explaining why it can be small at the plateau region.

V. CONCLUSIONS

By investigating the low-frequency (0.5–600 kHz) dielectric properties of CCTO over a large temperature range (90–500 K), we have proposed an explicit formula to fit the temperature dependence of the dielectric permittivity at different frequencies. Our statistical model can explain the low-temperature step-function-like dielectric relaxation of CCTO, estimate the activation energy of polarons, and shows that the permittivity plateau arises from the balance between the population and the polarizability of active polarons. The contribution from conductive charge carriers at high temperatures also plays a key role in the dielectric behavior. Our model and the fitting results provide a better understanding of the behavior of CCTO resulting from the interplay between the localization and conduction of charge carriers.

ACKNOWLEDGMENTS

This work was financially supported by the National Natural Science Foundation of China (NSFC), Grants No. 11564010, No. 11574246, No. U1537210, No. 51402196, and No. 51602159, the National Basic Research Program of China, Grant No. 2015CB654903, and the Natural Science Foundation of Guangxi (Grants No. GA139008, No. AA138162, No. AA294014, No. CB380006, and No. FA198015). A.A.B. and Z.G.Y. would like to thank the U. S. Office of Naval Research (Grants No. N00014-12-1-1045 and No. N00014-16-1-3106) and the Natural Sciences and Engineering Research Council of Canada (NSERC, Grant No. 203773) for support. D.W. also thanks the support from the China Scholarship Council (CSC No. 201706285020).

[1] M. A. Subramanian, L. Dong, N. Duan, B. A. Reisner, and A. W. Sleight, High dielectric constant in $ACu_3Ti_4O_{12}$ and $ACu_3Ti_3FeO_{12}$ phases, J. Solid State Chem. **151**, 323 (2000).

[2] A. P. Ramirez, M. A. Subramanian, M. Gardel, G. Blumberg, D. Li, T. Vogt, and S. M. Shapiro, Giant dielectric constant response in a copper-titanate, Solid State Commun. **115**, 217 (2000).

[3] C. C. Homes, T. Vogt, S. M. Shapiro, S. Wakimoto, and A. P. Ramirez, Optical response of high-dielectric-constant perovskite-related oxide, Science **293**, 673 (2001).

[4] Y. Lin, Y. B. Chen, T. Garret, S. W. Liu, C. Chen, L. Chen, R. P. Bontchev, A. Jacobson, J. C. Jiang, E. I. Meletis, J. Horwitz, and H.-D. Wu, Epitaxial growth of dielectric $CaCu_3Ti_4O_{12}$ thin films on (001) $LaAlO_3$ by pulsed laser deposition, Appl. Phys. Lett. **81**, 631 (2002).

[5] W. Si, E. M. Cruz, P. D. Johnson, P. W. Barnes, P. Woodward, and A. P. Ramirez, Epitaxial thin films of the giant-dielectric-constant material $CaCu_3Ti_4O_{12}$ grown by pulsed-laser deposition, Appl. Phys. Lett. **81**, 2056 (2002).

[6] A. A. Felix, M. O. Orlandi, and J. A. Varela, Schottky-type grain boundaries in CCTO ceramics, Solid State Commun. **151**, 1377 (2011).

[7] R. Schmidt, M. C. Stennett, N. C. Hyatt, J. Pokorny, J. Prado-Gonjal, M. Li, and D. C. Sinclair, Effects of sintering temperature on the internal barrier layer capacitor (IBLC) structure in $CaCu_3Ti_4O_{12}$ (CCTO) ceramics, J. Eur. Ceram. Soc. **32**, 3313 (2012).

[8] F. Han, S. Ren, J. Deng, T. Yan, X. Ma, B. Peng, and L. Liu, Dielectric response mechanism and suppressing high-frequency dielectric loss in Y_2O_3 grafted $CaCu_3Ti_4O_{12}$ ceramics, J. Mater. Sci.: Mater. Electron. **28**, 17378 (2017).

[9] J. Deng, X. Sun, S. Liu, L. Liu, T. Yan, L. Fang, and B. Elouadi, Influence of interface point defect on the dielectric properties of Y doped $CaCu_3Ti_4O_{12}$ ceramics, J. Adv. Dielect. **6**, 1650009 (2016).

[10] J. Deng, L. Liu, X. Sun, S. Liu, T. Yan, L. Fang, and B. Elouadi, Dielectric relaxation behavior and mechanism of $Y_{2/3}Cu_3Ti_4O_{12}$ ceramic, Mater. Res. Bull. **88**, 320 (2017).

[11] K. P. Neupane, J. L. Cohn, H. Terashita, and J. J. Neumeier, Doping dependence of polaron hopping energies in $La_{1-x}Ca_xMnO_3 (0 \leqslant x \leqslant 0.15)$, Phys. Rev. B **74**, 144428 (2006).

[12] R. S. Freitas, J. F. Mitchell, and P. Schiffer, Magnetodielectric consequences of phase separation in the colossal magnetoresistance manganite $Pr_{0.7}Ca_{0.3}MnO_3$, Phys. Rev. B **72**, 144429 (2005).

[13] C. Wang, Y. Cui, and L. Zhang, Dielectric properties of $TbMnO_3$ ceramics, Appl. Phys. Lett. **90**, 012904 (2007).

[14] A. Yang, Y. Sheng, M. A. Farid, H. Zhang, X. Lin, G. Li, L. Liu, F. Liao, and J. Lin, Copper doped $EuMnO_3$: synthesis, structure and magnetic properties, RSC Adv. **6**, 13928 (2016).

[15] J. Deng, M. A. Farid, A. Yang, J. Zhang, H. Zhang, L. Zhang, Y. Qiu, M. Yu, H. Zhu, M. Zhong, J. Li, G. Li, L. Liu, J. Sun, and J. Lin, The origin of multiple magnetic and dielectric anomalies of Mn-doped $DyMnO_3$ in low temperature region, J. Alloys Compd. **725**, 976 (2017).

[16] G. Li, Z. Chen, X. Sun, L. Liu, L. Fang, and B. Elouadi, Electrical properties of $AC_3B_4O_{12}$-type perovskite ceramics with different cation vacancies, Mater. Res. Bull. **65**, 260 (2015).

[17] T. Park, Z. Nussinov, K. R. A. Hazzard, V. A. Sidorov, A. V. Balatsky, J. L. Sarrao, S. Cheong, M. Hundley, J. Lee, Q. Jia, and J. Thompson, Novel Dielectric Anomaly in the Hole-Doped $La_2Cu_{1-x}Li_xO_4$ and $La_{2-x}Sr_xNiO_4$ Insulators: Signature of an Electronic Glassy State, Phys. Rev. Lett. **94**, 017002 (2005).

[18] J. Rivas, B. Rivas-Murias, A. Fondado, J. Mira, and M. A. Senaris-Rodriguez, Dielectric response of the charge-ordered two-dimensional nickelate $La_{1.5}Sr_{0.5}NiO_4$, Appl. Phys. Lett. **85**, 6224 (2004).

[19] J. Wu, C. Nan, Y. Lin, and Y. Deng, Giant Dielectric Permittivity Observed in Li and Ti Doped NiO, Phys. Rev. Lett. **89**, 217601 (2002).

[20] Y. Li, L. Fang, L. Liu, Y. Huang, and C. Hu, Giant dielectric response and charge compensation of Li- and Co-doped NiO ceramics, Mater. Sci. Eng., B **177**, 673 (2012).

[21] S. Ke, P. Lin, H. Fan, H. Huang, and X. Zeng, Variable-range-hopping conductivity in high-k $Ba(Fe_{0.5}Nb_{0.5})O_3$ ceramics, J. Appl. Phys. **114**, 104106 (2013).

[22] S. Ke, P. Lin, H. Huang, H. Fan, and X. Zeng, Mean-field approach to dielectric relaxation in giant dielectric constant perovskite ceramics, J. Ceram. **2013**, 795827 (2013).

[23] Y. Huang, D. Shi, L. Liu, G. Li, S. Zheng, and L. Fang, High-temperature impedance spectroscopy of $BaFe_{0.5}Nb_{0.5}O_3$ ceramics doped with $Bi_{0.5}Na_{0.5}TiO_3$, Appl. Phys. A **114**, 891 (2014).

[24] S. Liu, X. Sun, B. Peng, H. Su, Z. Mei, Y. Huang, J. Deng, C. Su, L. Fang, and L. Liu, Dielectric properties and defect mechanisms of $(1-x)Ba(Fe_{0.5}Nb_{0.5})O_3-xBiYbO_3$ ceramics, J. Electroceram. **37**, 137 (2016).

[25] X. Sun, J. Deng, S. Liu, T. Yan, B. Peng, W. Jia, Z. Mei, H. Su, L. Fang, and L. Liu, Grain boundary defect compensation in Ti-doped $BaFe_{0.5}Nb_{0.5}O_3$ ceramics, Appl. Phys. A **122**, 864 (2016).

[26] C. Wang and L. Zhang, Polaron relaxation related to localized charge carriers in $CaCu_3Ti_4O_{12}$, Appl. Phys. Lett. **90**, 142905 (2007).

[27] L. Zhang and Z. J. Tang, Polaron relaxation and variable-range-hopping conductivity in the giant-dielectric-constant material $CaCu_3Ti_4O_{12}$, Phys. Rev. B **70**, 174306 (2004).

[28] A. Tselev, C. M. Brooks, S. M. Anlage, H. Zheng, L. Salamanca-Riba, R. Ramesh, and M. A. Subramanian, Evidence for power-law frequency dependence of intrinsic dielectric response in the $CaCu_3Ti_4O_{12}$, Phys. Rev. B **70**, 144101 (2004).

[29] Z. Valdez-Nava, S. Guillemet-Fritsch, C. Tenailleau, T. Lebey, B. Durand, and J. Chane-Ching, Colossal dielectric permittivity of $BaTiO_3$-based nanocrystalline ceramics sintered by spark plasma sintering, J. Electroceram. **22**, 238 (2009).

[30] S. Vangchangyia, T. Yamwong, E. Swatsitang, P. Thongbai, and S. Maensiri, Selectivity of doping ions to effectively improve dielectric and non-Ohmic properties of $CaCu_3Ti_4O_{12}$ ceramics, Ceram. Int. **39**, 8133 (2013).

[31] R. Lohnert, H. Bartsch, R. Schmidt, B. Capraro, and J. Topfer, Microstructure and electric properties of $CaCu_3Ti_4O_{12}$ multilayer capacitors, J. Am. Ceram. Soc. **98**, 141 (2015).

[32] Y. Li, W. Li, G. Du, and N. Chen, Low temperature preparation of $CaCu_3Ti_3O_{12}$ ceramics with high permittivity and low dielectric loss, Ceram. Int. **43**, 9178 (2017).

[33] L. Liu, H. Fan, L. Wang, X. Chen, and P. Fang, Dc-bias-field-induced dielectric relaxation and ac conduction in $CaCu_3Ti_4O_{12}$ Ceramics, Philos. Mag. **88**, 537 (2008).

[34] L. Liu, D. Shi, S. Zheng, Y. Huang, S. Wu, Y. Li, L. Fang, and C. Hu, Polaron relaxation and non-Ohmic behavior in $CaCu_3Ti_4O_{12}$ ceramics with different cooling methods, Mater. Chem. Phys. **139**, 844 (2013).

[35] O. Bidault, M. Maglione, M. Actis, M. Kchikech, and B. Salce, Polaronic relaxation in perovskites, Phys. Rev. B **52**, 4191 (1995).

[36] N. F. Mott and E. A. Davis, *Electronic Processes in Non-crystalline Solids* (Clarendon, Oxford, UK, 1979).

[37] S. Krohns, P. Lunkenheimer, S. G. Ebbinghaus, and A. Loidl, Colossal dielectric constants in single-crystalline and ceramic $CaCu_3Ti_4O_{12}$ investigated by broadband dielectric spectroscopy, J. Appl. Phys. **103**, 084107 (2008).

[38] S. Y. Chung, I. D. Kim, and S. Kang, Strong nonlinear current-voltage behaviour in perovskite-derivative calcium copper titanate, Nat. Mater. **3**, 774 (2004).

[39] M. A. Kastner, R. J. Birgeneau, C. Y. Chen, Y. M. Chiang, D. R. Gabbe, H. P. Jenssen, T. Junk, C. J. Peter, P. J. Picone, T. Thio, T. R. Thurston, and H. L. Tuller, Resistivity of nonmetallic $La_{2-y}Sr_yCu_{1-x}Li_xO_{4-\delta}$ single crystals and ceramics, Phys. Rev. B **37**, 111 (1988).

[40] C. Ang, Z. Jing, and Z. Yu, Variable-range-hopping conduction and metal-insulator transition in Cu-doped $BaTiO_3$, J. Phys.: Condens. Matter **11**, 9703 (1999).

[41] A. Karmakar, S. Majumdar, and S. Giri, Polaron relaxation and hopping conductivity in $LaMn_{1-x}Fe_xO_3$, Phys. Rev. B **79**, 094406 (2009).

[42] J. Liu, F. Li, Y. Zeng, Z. Jiang, L. Liu, D. Wang, Z. Ye, and C. Jia, Insights into the dielectric response of ferroelectric relaxors from statistical modeling, Phys. Rev. B **96**, 054115 (2017).

[43] I. P. Raevski, S. A. Prosandeev, S. A. Bogatina, M. A. Malitskaya, and L. Jastrabik, High-k ceramic materials based on nonferroelectric $AFe_{1/2}B_{1/2}O_3$ (A-Ba, Sr, Ca; B-Nb, Ta, Sb) perovskites, Integr. Ferroelectr. **55**, 757 (2003).

[44] I. P. Raevski, S. A. Prosandeev, A. S. Bogatin, M. A. Malitskaya, and L. Jastrabik, High dielectric permittivity in $AFe_{1/2}B_{1/2}O_3$ nonferroelectric perovskite ceramics (A = Ba, Sr, Ca; B = Nb, Ta, Sb), J. Appl. Phys. **93**, 4130 (2003).

[45] Z. Abdelkafi, N. Abdelmoula, H. Khemakhem, O. Bidault, and M. Maglione, Dielectric relaxation in $BaTi_{0.85}(Fe_{1/2}Nb_{1/2})_{0.15}O_3$ perovskite ceramic, J. Appl. Phys. **100**, 114111 (2006).

[46] B. S. Kang, S. K. Choi, and C. H. Park, Diffuse dielectric anomaly in perovskite-type ferroelectric oxides in the temperature range of 400–700 °C, J. Appl. Phys. **94**, 1904 (2003).

[47] D. Ming, J. M. Reau, J. Ravez, J. Gitae, and P. Hagenmuller, Impedance-spectroscopy analysis of $LiTaO_3$-type single crystal, J. Solid State Chem. **116**, 185 (1995).

[48] S. O. Kasap, *Principles of Electronic Materials and Devices*, 3rd ed. (McGraw-Hill, New York, 2006).

[49] A. K. Jonscher, A new understanding of the dielectric relaxation of solids, J. Mater. Sci. **16**, 2037 (1981).

[50] M. Maglione, Free charge localization and effective dielectric permittivity in oxides, J. Adv. Dielectr. **6**, 1630006 (2016).

[51] L. Liu, S. Ren, J. Zhang, B. Peng, L. Fang, and D. Wang, Revisiting the temperature-dependent dielectric permittivity of $Ba(Ti_{1-x}Zr_x)O_3$, J. Am. Ceram. Soc. **101**, 2408 (2018).

[52] M. Sebastian and H. Jantunen, Low-loss dielectric materials for LTCC applications: a review, Int. Mater. Rev. **53**, 57 (2008).

[53] B. Barbier, C. Combettes, S. Guillemet-Fritsch, T. Chartier, F. Rossignol, and A. Rumeau, $CaCu_3Ti_4O_{12}$ ceramics from co-precipitation method: Dielectric properties of pellets and thick films, J. Eur. Ceram. Soc. **29**, 731 (2009).

[54] For X8R and X9R, the change of dielectric permittivity should be less than ±15% in a temperature range of −55 to 150 °C and —55 to 200 °C, respectively.

[55] P. Krissana, S. Ekaphan, and P. Thanin, Ultra-stable X9R type $CaCu_{3-x}Zn_xTi_4O_{12}$ ceramics, Ceram. Int. **44**, 20739 (2018).

[56] J. Jumpatam, B. Putasaeng, T. Yamwong, P. Thongbai, and S. Maensiri, A novel strategy to enhance dielectric performance and non-Ohmic properties in $Ca_2Cu_{2-x}Mg_xTi_4O_{12}$, J. Eur. Ceram. Soc. **34**, 2941 (2014).

[57] C. Ang, Z. Yu, and L. E. Cross, Oxygen-vacancy-related low-frequency dielectric relaxation and electrical conduction in Bi : $SrTiO_3$, Phys. Rev. B **62**, 228 (2000).